J Mater Sci (2009) 44:3049–3056
DOI 10.1007/s10853-009-3403-1

Effects of samarium on microstructure and mechanical properties of Mg–Y–Sm–Zr alloys during thermo-mechanical treatments

Daquan Li · Qudong Wang · Wenjiang Ding

Received: 20 August 2007 / Accepted: 16 March 2009 / Published online: 3 April 2009

Abstract Microstructure and mechanical properties of Mg–4Y–*x*Sm–0.5Zr ($x = 1, 4, 8$) alloys during thermo-mechanical treatments were investigated in this study. Mg–4Y–4Sm–0.5Zr alloy exhibits higher tensile strength but lower elongation than Mg–4Y–1Sm–0.5Zr alloy during the thermo-mechanical treatments. Large amount of intermetallic phases still remained at grain boundaries in Mg–4Y–8Sm–0.5Zr alloy after solution. These undissolved phases can strengthen the grain boundaries at temperatures higher than 573 K. But the room temperature mechanical properties of Mg–4Y–8Sm–0.5Zr alloy during the thermo-mechanical treatments were greatly weakened for the brittleness of these undissolved intermetallic phases.

Introduction

Magnesium is the lightest of all metals used as the basis for constructional alloys [1]. There has been a rapid growth in interest in the development of magnesium alloys for their good characteristic properties like low density, good damping capacity, high specific strength/stiffness, diecastability, dimensional stability, machinability and low casting cost [2–4].

It has been demonstrated that rare earth metals (RE) are the most effective elements to improve the strength properties of magnesium especially at elevated temperatures [5–8]. One important group of Mg–RE alloys, based on the Mg–Y–Nd system, identified as WE54 (5 wt% Y, 3.3 wt% RE, 0.5 wt% Zr) and WE43 (4 wt% Y, 3.3 wt% RE, 0.5 wt% Zr), are those strengthened essentially by precipitation hardening [6, 9–11]. The precipitation sequence in WE series alloys has been reported to involve formation of phases designated β'', β', β_1 and β [3, 12–14]. Furthermore, the mechanical properties of these Mg–RE alloys can be further improved by thermo-mechanical treatments because of the grain refinement and accelerated precipitation [6, 15].

The maximum solubility of samarium in solid magnesium at eutectic temperature 815 K is 5.8 wt%, which is larger than that of neodymium (3.6 wt%), and it has been proved that the solution and precipitation strengthening effects of samarium is higher than that of neodymium in magnesium alloys [16]. A recently developed Mg–4Y–4Sm–0.5Zr alloy exhibits more attractive properties than the widely used WE series alloys [17]. Further investigation of this alloy shows that the optimal mechanical properties of the alloy achieved after solution at 798 K for 8 h and then under-aged at 473 K for 16 h [18].

In this study, thermo-mechanical treatments containing solution, artificial ageing and extrusion were carried out on three kinds of Mg–4Y–*x*Sm–0.5Zr ($x = 1, 4, 8$) alloys to further increase the mechanical properties of the alloys. The Y content in these three alloys is chosen as 4 wt%, which is close to that in WE series alloys. Three alloys with low Sm content as 1 wt% (much lower than the maximum solubility of Sm in solid magnesium), medium Sm content

D. Li (✉)
National Engineering Research Center for Nonferrous Metals Compositions, General Research Institute for Nonferrous Metals (GRINM), No. 2 Xinjiekou Wai Street, 100088 Beijing, People's Republic of China
e-mail: lidaquan1121@yahoo.cn

D. Li · Q. Wang · W. Ding
National Engineering Research Center of Light Alloys Net Forming, School of Materials Science and Engineering, Shanghai Jiaotong University, 800 Dongchuan Road, 200240 Shanghai, People's Republic of China

as 4 wt% (close to the maximum solubility of Sm in solid magnesium) and high Sm content as 8 wt% (much higher than the maximum solubility of Sm in solid magnesium) were investigated to evaluate the effects of samarium on microstructure and mechanical properties of Mg–4Y–*x*Sm–0.5Zr alloys. The results indicate that the amount of samarium has strong effects on both microstructure evolution and mechanical properties of the alloys during the thermo-mechanical treatments.

Experimental method

The chemical compositions of studied Mg–Y–Sm–Zr alloys are listed in Table 1. The practical chemical compositions of these alloys were analyzed by inductively coupled plasma.

The alloys were solution treated at 798 K for 8 h followed by quenching in cold water. After solution treatment, the alloys were isothermally aged at 448, 473 and 498 K for different times in the oil-bath. The ageing responses of the alloys were checked by hardness measurement. Hardness was measured with a Vickers-hardness tester under a load of 30 kg. Extrusion of the solution-treated alloys was carried out at 623 K with extrusion ratio 10:1. Extruded alloys were then aged at 473 K for different times.

The microstructure of the alloys was analyzed by light microscope (OM, LEICA MEF4M). The specimens were mechanically polished and etched with a dilute solution of 4% nitric acid in alcohol. The average grain size was measured by the linear intercept method. The room temperature tensile properties were tested on Zwick/Roell testing machine, and the high temperature tensile tests were carried out on Shimadzu machine at an initial strain rate of 10^{-3} s^{-1} at different temperatures from 423 to 623 K. The tensile specimens have a gauge length of 10 mm, a gauge width of 3.5 mm and a gauge thickness of 2 mm.

Experimental results

Microstructure

Figure 1 shows the microstructure of the as-cast Mg–Y–Sm–Zr alloys. The average grain size of the alloy 1, 2 and 3 is 62, 50 and 44 μm, respectively. The grain size of the as-cast Mg–Y–Sm–Zr alloys decreases, and the amount of eutectic phases at grain boundaries increases in the sequence of alloys 1–3.

Table 1 Chemical composition (wt%) of Mg–Y–Sm–Zr alloys

Nominal alloy	Y	Sm	Zr	Mg
Alloy 1	4.61	1.48	0.50	Bal.
Alloy 2	3.98	3.78	0.49	Bal.
Alloy 3	4.51	8.45	0.42	Bal.

Figure 2 shows the microstructure of the solution-treated Mg–Y–Sm–Zr alloys. The average grain size of the solution-treated alloys 1, 2 and 3 is 65, 61 and 45 μm, respectively. The eutectic phases in alloys 1 and 2 were dissolved into the Mg matrix after solution treatment, and the average grain size of the solution-treated alloys 1 and 2 became a little larger than that of the as-cast alloys. There was still large amount of second phases remained at grain boundaries in solution-treated alloy 3, and there was no evident grain growth occurred in alloy 3 after solution treatment.

Figure 3 shows the microstructure of the extruded Mg–Y–Sm–Zr alloys. As can be seen from Fig. 3, the grains of Mg–Y–Sm–Zr alloys were greatly refined during the extrusion process. Especially, the grain size of alloy 3 is much smaller than that of alloys 1 and 2 after extrusion. The longitudinal microstructure of the extruded alloy 3 is shown in Fig. 3d. The intermetallic particles are distributed along the extrusion direction after extrusion.

Hardness curves

The results of hardness evolution of the solution-treated Mg–Y–Sm–Zr alloys during isothermal ageing at 448, 473 and 498 K are presented in Fig. 4. The hardness of the solution-treated alloys increases in the sequence of alloys 1–3. In alloy 1, two stages [16] are demonstrated evidently in the hardness curves. At the first stage, hardness increases slowly with increasing ageing time, and then remains approximately at a constant level. At the second stage (after 32 h), hardness begins to ascend steeply, reaches the maximum and then descends after maximum with increasing ageing time. Alloy 1 needs much longer ageing times than the other two alloys to reach the maximum hardness at the same ageing temperatures. Alloys 2 and 3 represent the similar ageing behaviours except the starting hardness. The hardness increases at the beginning, and continues gradually up to the maximum, then falls down with increasing ageing time. Only one stage [16] is seen clearly in these two alloys. These two alloys need almost the same time to reach the maximum hardness at the same ageing temperatures. And the hardness enhancement of these two alloys between the starting hardness and the maximum one at the same ageing temperatures is nearly the same.

Figure 5 shows the results of hardness evolution of the extruded Mg–Y–Sm–Zr alloys during isothermal ageing at 473 K. The hardness of alloys 1 and 2 in the as-extruded state is evidently higher than that before

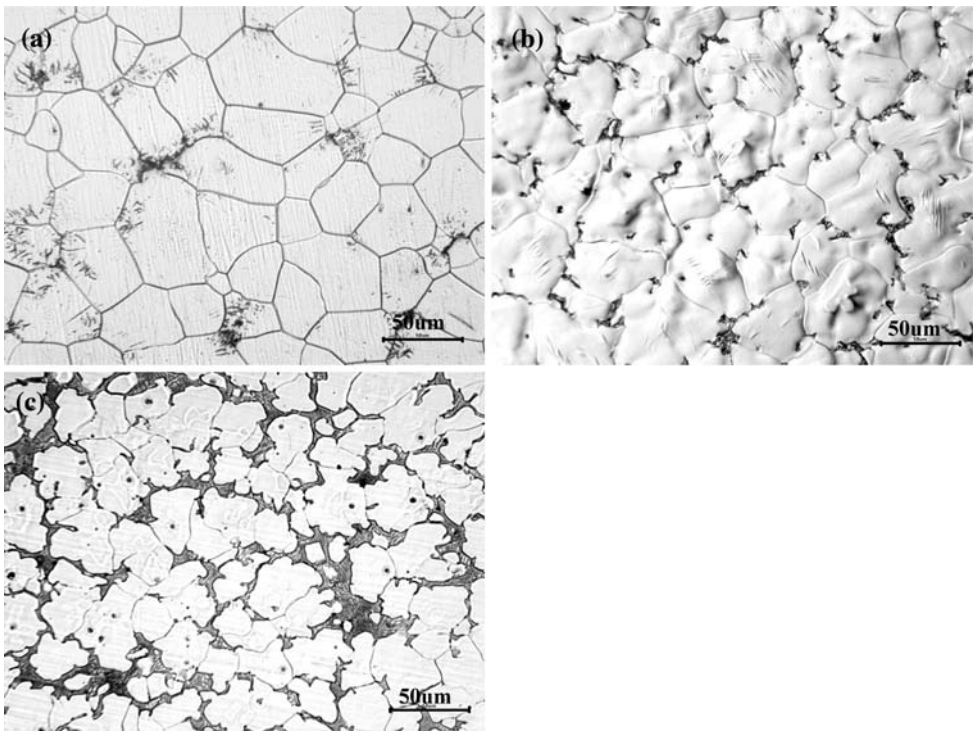

Fig. 1 Optical micrographs of as-cast Mg–Y–Sm–Zr alloys: **a** alloy 1, **b** alloy 2 and **c** alloy 3

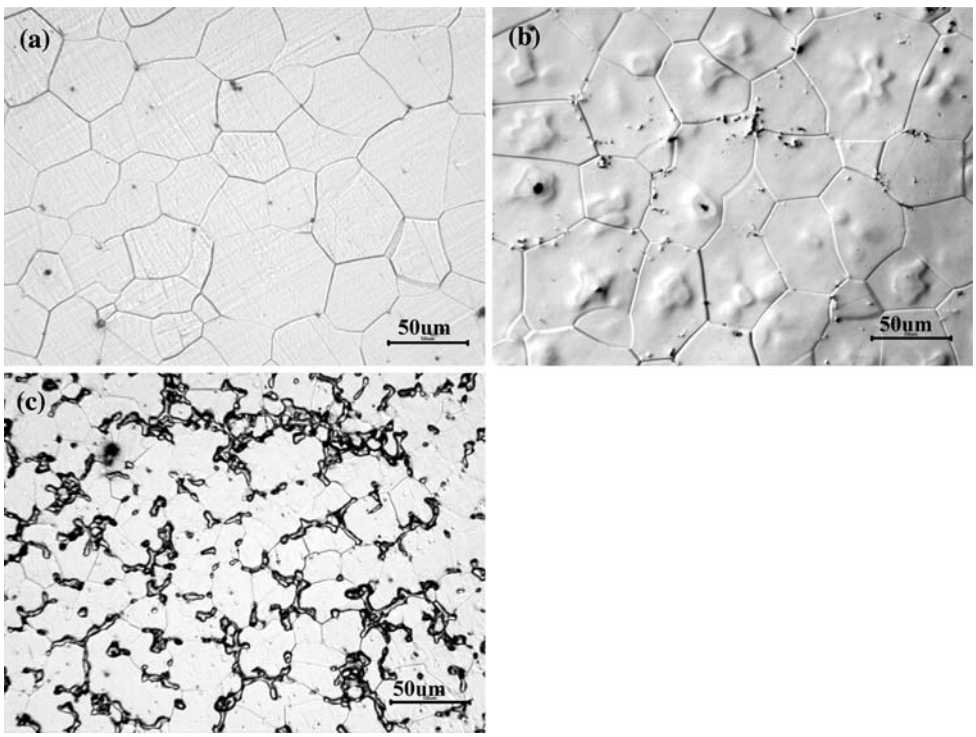

Fig. 2 Optical micrographs of the solution-treated Mg–Y–Sm–Zr alloys: **a** alloy 1, **b** alloy 2 and **c** alloy 3

extrusion. The alloys need shorter ageing times to reach the maximum hardness in the as-extruded state than in the solution-treated state, but the enhancement between the starting hardness and the maximum one weakened after extrusion.

Tensile properties

Figure 6 shows the tensile properties of the as-cast Mg–Y–Sm–Zr alloys. The yield strength (YS) increases and the elongation (EL) decreases in the sequence of alloys 1–3.

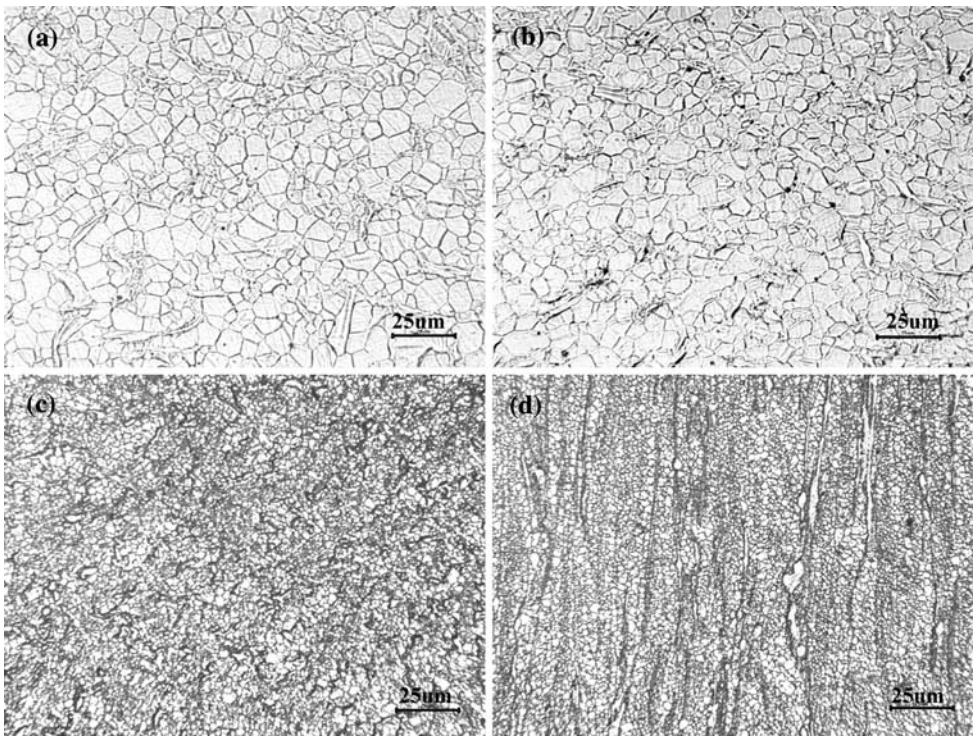

Fig. 3 Optical micrographs of extruded Mg–Y–Sm–Zr alloys: **a** alloy 1 in transverse section, **b** alloy 2 in transverse section, **c** alloy 3 in transverse section and **d** alloy 3 in longitudinal section

The ultimate tensile strength (UTS) of alloys 1 and 2 is nearly the same. And the UTS and YS of alloy 3 are obviously higher than that of alloys 1 and 2.

Figure 7 shows the tensile properties of the solution-treated Mg–Y–Sm–Zr alloys. The EL of alloys 1 and 2 greatly increases after solution. And alloy 2 exhibits higher UTS and YS but lower EL than alloy 1 after solution. There are no evident changes in ELs of alloy 3 between as-cast and solution-treated state. But the YS and UTS of alloy 3 decrease after solution.

Figure 8 shows the tensile properties of Mg–Y–Sm–Zr alloys after solution-plus-ageing heat treatment. The UTS and YS of alloys 1 and 2 greatly increase but the EL of these two alloys decrease after this solution-plus-ageing heat treatment. And alloy 2 still exhibits higher UTS and YS, but lower EL than alloy 1 after solution-plus-ageing heat treatment. The YS evidently increases, but the UTS and EL of alloy 3 keep almost the same after the solution-plus-ageing heat treatment.

High temperature tensile properties of Mg–Y–Sm–Zr alloys after solution-plus-ageing heat treatment are shown in Fig. 9. The UTS of these three alloys keeps almost the same until 473 K. Then, the strength decreases steeply at test temperatures higher than 523 K. And alloy 3 exhibits the highest UTS at 573 and 623 K. The EL of all three alloys increases with increasing the test temperatures, but the EL increase of alloy 3 is not evident.

Figure 10 shows the tensile properties of the extruded Mg–Y–Sm–Zr alloys. The UTS, YS and EL of alloys 1 and 2 greatly increase after extrusion. And alloy 2 exhibits higher UTS and YS, but lower EL than alloy 1 in the as-extruded state.

Figure 11 shows the tensile properties of extruded Mg–Y–Sm–Zr alloys after ageing. The YS and UTS of both alloys increase greatly after ageing heat treatment, but the EL decreases consequently. Alloy 2 exhibits higher UTS and YS but lower EL than alloy 1 after ageing just as in the as-extruded state.

Discussion

The amount of eutectic phases in as-cast Mg–Y–Sm–Zr alloys increases while the grain size decreases with increasing Sm content. Samarium has an effect on grain refinement of as-cast Mg–Y–Sm–Zr alloys. The YS of as-cast alloys increases while the EL decreases in the sequence of alloys 1–3. This is mainly due to the increasing amount of the eutectic phases. These eutectic phases at the grain boundaries may effectively block the dislocation slip and promote a substantial strengthening effect in the alloys. But they may also become the crack sources during the tensile test, so the EL of the alloys decreases.

The EL of alloys 1 and 2 heavily increases after solution for the complete dissolution of the fragile eutectic phases and the homogenous distribution of the alloying elements during the solution process [18]. The UTS and YS of alloy 2 are a little higher than that of alloy 1 in the solution-

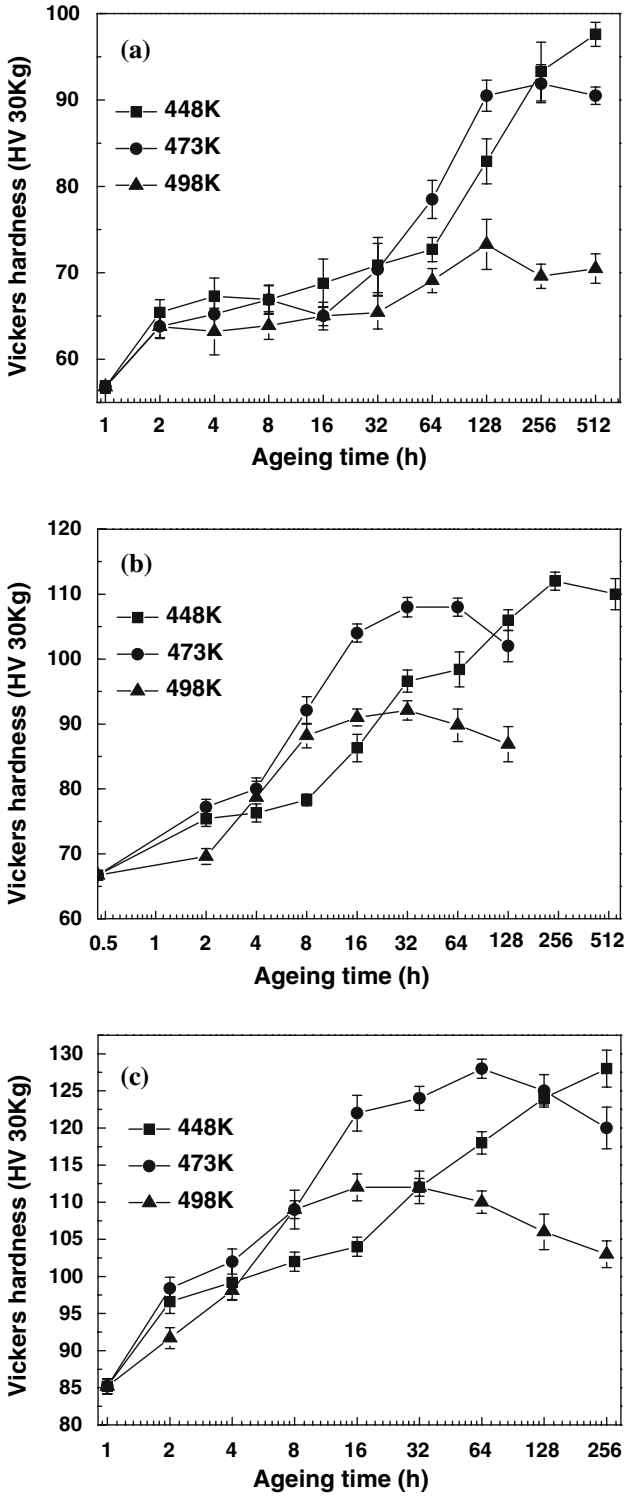

Fig. 4 Hardness evolution of the solution-treated Mg–Y–Sm–Zr alloys during isothermal ageing at 448, 473 and 498 K: **a** alloy 1, **b** alloy 2, **c** alloy 3

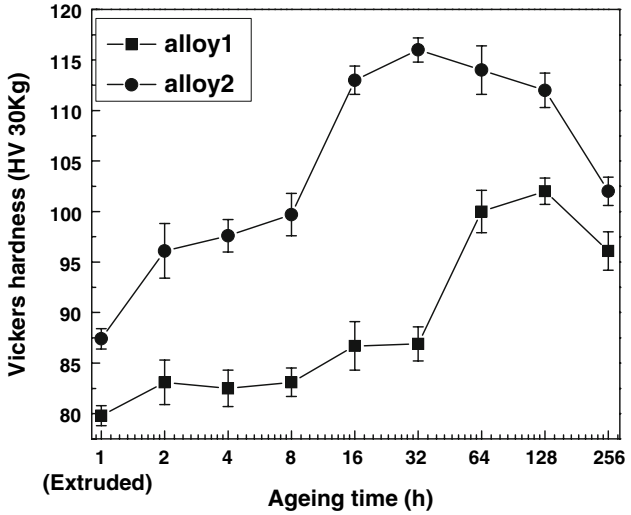

Fig. 5 Hardness evolution of extruded Mg–Y–Sm–Zr alloys during isothermal ageing at 473 K

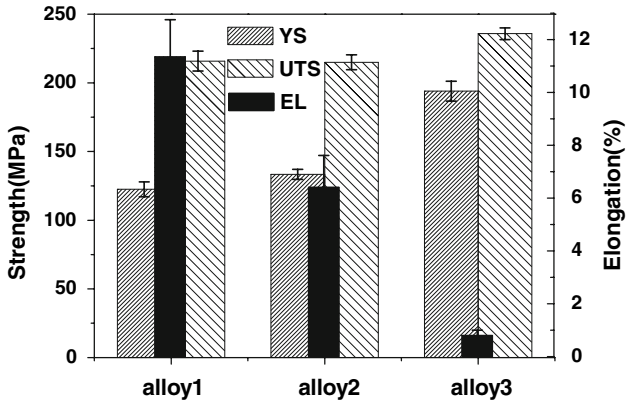

Fig. 6 Tensile properties of as-cast Mg–Y–Sm–Zr alloys

treated state. Since the difference between these two alloys is primarily the dissolved content of the samarium, it can be concluded that there has been some solution strengthening effects of samarium in the solution-treated Mg–Y–Sm–Zr alloys. The content of Sm in alloy 3 is 8.45 wt%, which is much larger than the maximum solubility of samarium in solid magnesium (5.8 wt%) [16]. There is still large amount of the second phases remained at grain boundaries in the solution-treated alloy 3 for the incomplete dissolution of the samarium. As a result, there is no evident solution strengthening effect in alloy 3.

Alloys 2 and 3 exhibit the very similar one stage ageing behaviours though they contain the much different Sm content. The content of Sm in alloy 3 is much larger than that in alloy 2, but a part of the Sm content in alloy 3 is enriched in the second phases, as a result, the solution content of Sm in alloy 3 is similar to that in alloy 2. It is reasonable that the two alloys exhibit the similar ageing behaviours for the similar solution content of Sm and Y in Mg matrix. Alloy 1 exhibits the completely different two stage ageing behaviours compared with alloys 2 and 3, and

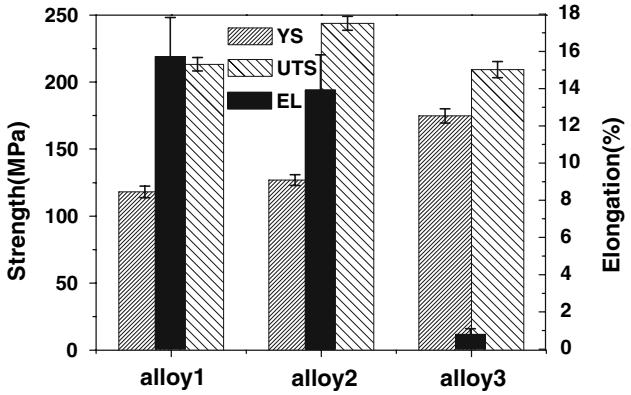

Fig. 7 Tensile properties of solution-treated Mg–Y–Sm–Zr alloys

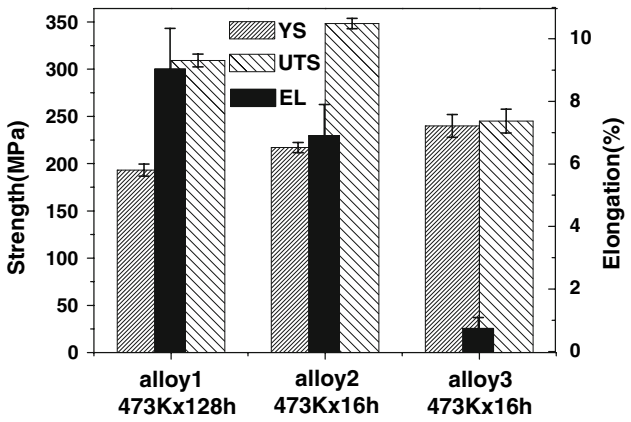

Fig. 8 Tensile properties of Mg–Y–Sm–Zr alloys after solution-plus-ageing heat treatment

alloy 1 needs much longer ageing times than the other two alloys to reach the maximum hardness at the same ageing temperatures. The possible reasons are: first, the supersaturation of Sm in Mg matrix in alloys 2 and 3 is much larger than that in alloy 1, so the decomposition is noticeably accelerated with increasing supersaturation, and the hardening effect also increases, respectively; second, the decomposition of Y may play the main strengthening effects in alloy 1 for the larger dissolution content of Y than Sm in the Mg matrix. This two stage ageing behaviour and the long ageing times are similar to the decomposition behaviours in the Mg–Y binary alloys [16].

The precipitation strengthening of the alloying elements Y and Sm is the main strengthening mechanism in these Mg–Y–Sm–Zr alloys. The mechanical properties of Mg–Y–Sm–Zr alloys greatly increased after the solution-plus-ageing heat treatment. Alloy 2 exhibits higher mechanical properties than alloy 1 after the heat treatment, for larger precipitation strengthening effect of Sm resulting from the lager Sm content in alloy 2. But the precipitation strengthening effect in alloy 3 is weakened for the brittleness of the alloy.

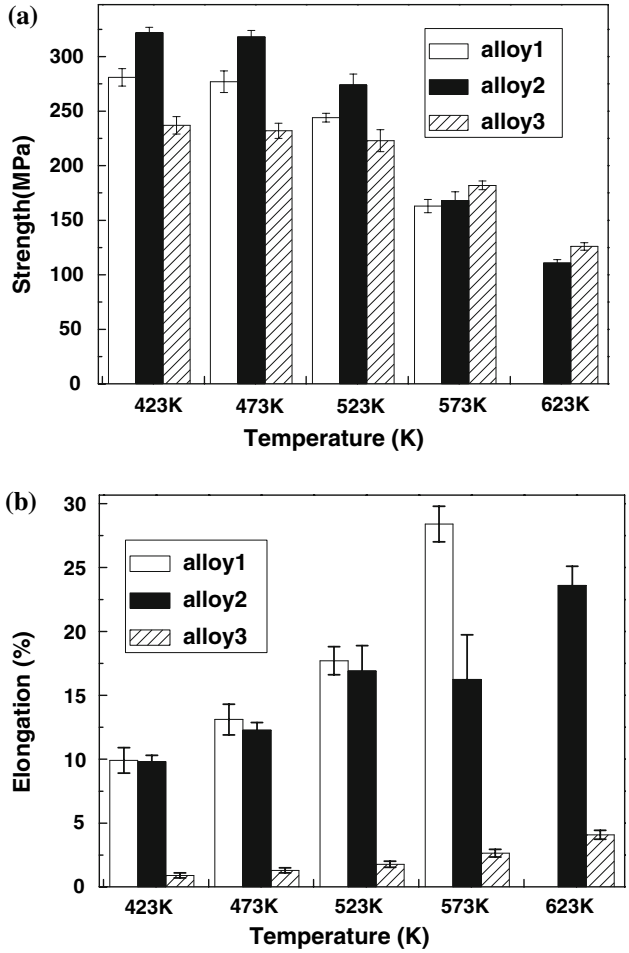

Fig. 9 High temperature UTS and EL of Mg–Y–Sm–Zr alloys after solution-plus-ageing heat treatment: **a** UTS, **b** EL, alloy 1 was aged at 473 K for 128 h, alloy 2 was aged at 473 K for 48 h and alloy 3 was aged at 473 K for 16 h

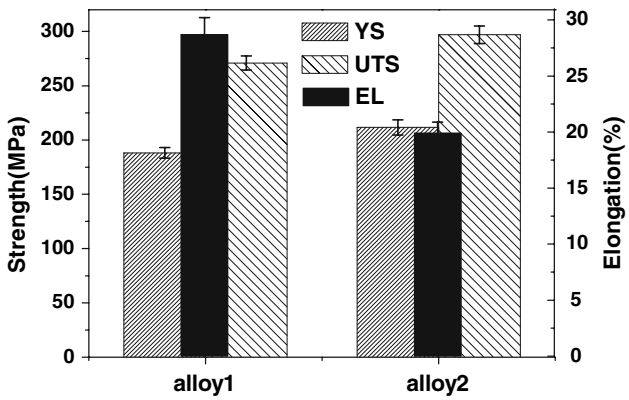

Fig. 10 Tensile properties of extruded Mg–Y–Sm–Zr alloys

The tensile strength of the Mg–Y–Sm–Zr alloys can hold up to 473 K, then decreases steeply at higher temperatures, for the softening of the precipitates and the

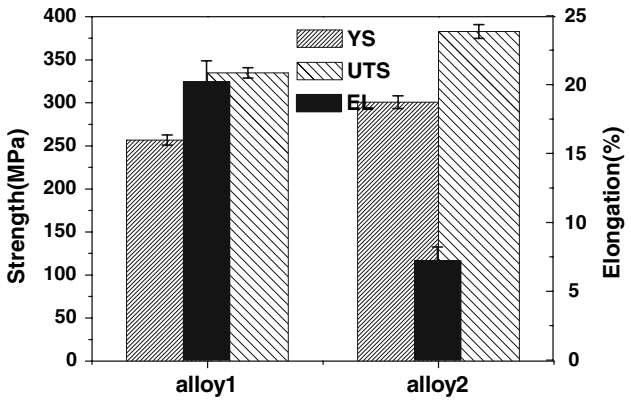

Fig. 11 Tensile properties of extruded Mg–Y–Sm–Zr alloys after ageing, alloy 1 was aged at 473 K for 96 h and alloy 2 was aged at 473 K for 16 h

activation of non-basal slip systems above 473 K [18]. And the softening of grain boundaries at high temperatures may also be an important factor. At temperatures higher than 573 K, it is alloy 3 that exhibits the highest ultimate tensile strength. And this may be because that the undissolved intermetallic phases at grain boundaries in alloy 3 can strengthen the grain boundaries and preventing the movement of large angle grain boundaries at high temperatures where the grain boundaries become weak.

Dynamic recrystallization (DRX) occurred in all the three alloys during the extrusion process. And the grain size of the alloys is greatly refined after extrusion. In alloy 3, the undissolved phases at grain boundaries may effectively restrain the DRX grain growth during hot extrusion, as a result, very fine DRX grains obtained in the as-extruded alloy 3. The mechanical properties of as-extruded alloys 1 and 2 increased evidently due to the very fine microstructure produced by extrusion. But alloy 3 cracked during extrusion for its serious brittleness. The precipitation strengthening effect of Y and Sm elements in the extruded alloys is also effective. There is a great enhancement of UTS and YS in extruded alloys after ageing. But the precipitation strengthening effect in these extruded alloys is somewhat lower than that in the solution-treated state. There might be dynamic precipitation in the alloys during the extrusion process. And the supersaturation degree of Y and Sm in Mg–Y–Sm–Zr alloys may decrease correspondingly after extrusion, as a result, the precipitation strengthening effect in the extruded alloys weakened. But the precipitation process accelerated in spite of the decreased degree of supersaturation, and this is mainly caused by the large amount of grain boundaries and dislocations introduced by extrusion, where the precipitates preferentially precipitated for their high interface energy.

Conclusions

The amount of eutectic phases in the as-cast Mg–Y–Sm–Zr alloys increases, and the grain size of the as-cast alloys decreases with the increasing Sm content. The YS increases while the EL decreases, respectively.

The solution and precipitation strengthening of the alloying elements Y and Sm is the main strengthening mechanism in these Mg–Y–Sm–Zr alloys. The strengthening effects of Sm in Mg–Y–Sm–Zr alloys increase, and the decomposition process of solution-treated Mg–Y–Sm–Zr alloys also accelerates with increasing the Sm content. The strengthening effects in alloy 3 are greatly weakened for the serious brittleness of the alloy.

The UTS decreases, but the EL increases with increasing the test temperatures in all the alloys. And alloy 3 exhibits the highest UTS when temperatures are higher than 573 K for the second phases, which remained at grain boundaries in alloy 3 that can strengthen the grain boundaries at high temperatures where they become weak.

The grains of alloys are evidently refined for the occurrence of DRX during extrusion process. The mechanical properties of alloys 1 and 2 greatly increased after extrusion-plus-ageing treatment for the combined strengthening effects of grain refinement and precipitation. Alloy 3 was cracked during extrusion process for the brittleness of the alloy.

Acknowledgements This work was supported by International Cooperation Fond of Shanghai Science and Technology Committee, Shanghai/Rhone-Alpes Science and Technology cooperation fund (No. 06SR07104).

References

1. Mordike BL, Ebert T (2001) Mater Sci Eng A 302:37
2. Aghion E, Gueta Y, Moscovitch N, Bronfin B (2008) J Mater Sci 43:4870. doi:10.1007/s10853-008-2708-9
3. Wang JG, Hsiung LM, Nieh TG, Mabuchi M (2001) Mater Sci Eng A 315:81
4. Li ZC, Zhang H, Liu L, Xu YB (2004) Mater Lett 58:3021
5. Peng Q, Wu Y, Fang D, Meng J, Wang L (2007) J Mater Sci 42:3908. doi:10.1007/s10853-006-0451-7
6. Mohri T, Mabuchi M, Satio N, Nakamura M (1998) Mater Sci Eng A 257:287
7. Weiss D, Kaya AA, Aghion E, Eliezer D (2002) J Mater Sci 37:5371. doi:10.1023/A:1021001813867537 1-5379
8. Song YL, Liu YH, Yu SR, Zhu XY, Wang SH (2007) J Mater Sci 42:4435. doi:10.1007/s10853-006-0661-z
9. Rokhlin LL, Dobatkina TV, Tarytina IE, Timofeev VN, Balakhchi EE (2004) J Alloy Compd 367:17
10. Nie JF, Muddle BC (1999) Scri Mater 40:1089
11. Nie JF, Xiao XL, Luo CP, Muddle BC (2001) Micron 32:857
12. Smola B, Stulikova I (2004) J Alloy Compd 381:L1

13. Ping DH, Hono K, Nie JF (2003) Scri Mater 48:1017
14. Nie JF, Muddle BC (2000) Acta Mater 48:1691
15. Nakashima K, Iwasaki H, Mori T, Mabuchi M, Nakamura M, Asahina T (2000) Mater Sci Eng A 293:15
16. Rokhlin LL (2003) In: Magnesium alloys containing rare earth meals. Taylor and Francis Inc., London
17. Li D, Wang Q, Ding W (2006) Mater Sci Eng A 428:295
18. Li D, Wang Q, Ding W (2007) Mater Sci Eng A 448:165